Synthesis of Gold Nanoparticles Capped-Benzoic Acid Derivative Compounds (*o*-, *m*-, and *p*-Hydroxybenzoic Acid)

Agustina Sus Andreani, Eko Sri Kunarti, and Sri Juari Santosa*

Department of Chemistry, Faculty of Mathematics and Natural Sciences, Universitas Gadjah Mada, Sekip Utara Yogyakarta 55281, Indonesia

** Corresponding author:*

tel: +62-8164262984
email: sjuari@ugm.ac.id

Received: March 29, 2018
Accepted: August 31, 2018

DOI: 10.22146/ijc.34440

Abstract: *The effect of a hydroxyl functional group of the benzoic acid derivative compound, i.e.* o-*hydroxybenzoic acid,* m-*hydroxybenzoic acid, and* p-*hydroxybenzoic acid on the synthesis of AuNPs has been studied. It was revealed that the pH, heating time, the concentration of capping agent and the concentration of* Au^{3+} *affected the formation of AuNPs. We discovered that* o-*hydroxybenzoic acid possessed the highest stability, yet it needed the highest concentration of* Au^{3+} *and faster reaction time than* p-*hydroxybenzoic acid and slower than* m-*hydroxybenzoic acid. The stability was verified by means of UV-Vis spectrophotometer, XRD, TEM, Particle Size Analyzer (PSA), and Zeta Potential with an aging time of more than 5 months. We concluded that* o-*hydroxybenzoic acid acquired the most effective redox reaction instead of* m-*hydroxybenzoic acid and* p-*hydroxybenzoic acid, resulted in the smaller sized and unaggregated AuNPs. We also confirmed that the hydroxyl group of* o-*hydroxybenzoic acid,* m-*hydroxybenzoic acid and* p-*hydroxybenzoic acid is the functional group responsible for the reduction of* Au^{3+} *to* Au^{0}.

Keywords: *AuNPs;* o-*hydroxybenzoic acid;* m-*hydroxybenzoic acid;* p-*hydroxybenzoic acid*

■ INTRODUCTION

The research on AuNPs including their synthesis, characterization, and application has been developed in recent years. Due to the unique properties of gold nanoparticle (AuNPs) which are different from its bulk form, AuNPs are used in several fields such as environment, medication, industries etc. One of the applications of AuNPs for the environmental purpose is heavy metals detection in water. For the next few years, Indonesia government is focusing on increasing the water quality by monitoring the concentration of heavy metals in water. Therefore, it is important to carry out prior research on heavy metal detection in Indonesia's water by developing a nano-sensor.

Recently, AuNPs were developed as a heavy metal sensor in the environment [1-3], yet most synthesized AuNPs are easily aggregated and its ability to function as sensor declines. Therefore, the challenge to find more precise and better method to synthesis AuNPs with high stability remains a big opportunity in nano-society. The AuNPs is generally synthesized through the reduction of the $HAuCl_4$ solution with $NaBH_4$ in high temperature [4]. However, the synthesized AuNPs tend to aggregate as soon as it is formed. The use of the other reducing agents, such as hydrazine, formaldehyde, hydroxylamine, saturated alcohols, citric acid, and hydrogen peroxide still could not solve the aggregation problem of AuNPs. Therefore, the synthesized AuNPs require a capping agent as a stabilizer to prevent collisions of its particles.

The most common capping agents used in previous studies were PVA [5], PEG [6], and surfactant [7]. Subsequently, the synthesis of AuNPs was developed by the addition of a stabilizing agent or capping agent after the reduction process to maintain the size of AuNPs. Kimling et al. synthesized AuNPs by capping Au^{3+} using a surfactant and then reducing using citric acid [8]. Citric acid was also used as a reducing agent for AuNPs and, Fitriyana and Kurniawan [9] added

polyaniline. Polyaniline-modified gold was used for sucrose detection. PVA was used as a capping agent for the synthesis of silver nanoparticles (AgNPs), which had been previously reduced with ascorbic acid [10]. However, the use of two different compounds was not effective.

In 2010, Indumathy et al. also synthesized AuNPs using thiosalicylic acid as both reducing agent and stabilizing agent [11]. Six years afterward, Gusrizal et al. and Gusrizal et al. had synthesized AgNPs using derivative compounds of benzoate (*o*-hydroxybenzoic acid, *m*-hydroxybenzoic acid, and *p*-hydroxybenzoic acid) as both reducing agents and capping agents to synthesize silver nanoparticles (AgNPs) [12-13]. It is reported that the derivative compounds of benzoate increased the stability of AgNPs for 5 months.

In this work, we carried out the synthesis of AuNP using $[AuCl_4]^-$ as the precursor and benzoic acid derivatives as the capping agents, inspired by Gusrizal's work on the synthesis of AgNPs using same capping agents [12-13]. The optimum $[AuCl_4]^-$ and capping agent concentration will be evaluated and the effect of different substituent positions, i.e. *o*-, *m*- and *p*-hydroxy group position on benzoic acid towards the shape and stability of synthesized nanoparticles will be examined and compared. It was expected that this study would lead to further development of synthesizing stable AuNPs by using hydroxybenzoic acid's derivatives, and the substituent effect would give valuable information for further exploration.

■ EXPERIMENTAL SECTION

Materials

Chemicals used in this research were commercially obtained from Merck, i.e. *o*-hydroxybenzoic acid, *p*-hydroxybenzoic acid, *m*-hydroxybenzoic acid, and sodium hydroxide. The pure gold bar (99.99%) was purchased from PT Antam Tbk. HCl 30% and H_2SO_4 were purchased from Mallinckrodt and HNO_3 was supplied by Merck. $HAuCl_4$ standard solution 100 mg/L was prepared by dissolving 0.1 g pure gold in 1000 mL of aqua regia solution (4 HCl: 1 HNO_3).

Instrumentation

The crystal structure of the materials was characterized by X-ray diffraction pattern at a scanning rate of 4 deg/min in 2θ in the range of 0° to 80°, using a Shimadzu XRD-6000 diffractometer equipped with monochromatic high-intensity Cu K_α radiation (λ = 0.15418) produced at 40 kV and 30 mA. Infrared spectra of samples were recorded on Shimadzu Prestige-21 infrared Spectrophotometer using solid KBr pellets to qualitatively investigate their related functional groups. Ultraviolet-visible spectra were recorded on Shimadzu S-600 UV-Vis spectrophotometer in the range of 300 to 600 nm. The TEM observations were carried out using JEM-1400 JEOL 120 kV. The Particle Size Analyzer (PSA) and zeta potential were determined using Horiba SZ-100.

Procedure

Synthesis of AuNPs

The synthesis of AuNPs was carried out according to Turkevich simple method [4] by mixing $HAuCl_4$ with capping agents (*o*-hydroxybenzoic acid, *m*-hydroxy benzoic acid, *p*-hydroxybenzoic acid) at a volume ratio 1:1 in a water bath at 98 °C with a variation of incubation times of 5 to 60 min [10-11]. Meanwhile, the concentrations of capping agents in this research were varied from 0.01 to 0.15 M and the concentrations of $HAuCl_4$ were varied from 10 to 100 ppm. The optimization of pH (1.0 to 12) was also conducted in this research to evaluate the effect of pH towards the synthesized product.

Characterization of AuNPs

The AuNPs at optimum conditions was centrifuged using Centrifuge Micro Thermo Sorvall LM17 at 15,000 rpm for 10 min. The formed solid was then dried at 50 °C for 2 h and was characterized using FTIR Spectrophotometer and XRD. Meanwhile, the un-centrifuged solution was characterized by TEM, Zeta Potential and Particle Size Analyzer (PSA).

■ RESULTS AND DISCUSSION

Optimization of Synthesis of AuNPs

Gold nanoparticles (AuNPs) in this research were formed because Au^{3+} was reduced to Au^0 by *o*-hydroxy benzoic acid, *m*-hydroxybenzoic acid or *p*-hydroxy benzoic acid. These compounds have lone pair electrons which can be donated to Au^{3+} to form Au^0. The compounds, *o*-hydroxybenzoic acid, *m*-hydroxybenzoic acid, and *p*-hydroxybenzoic acid, have two groups, i.e. hydroxyl and carboxylic which can donate lone pair electrons. One of them was expected to reduce Au^{3+} and the other act as a stabilizer to obtain stable AuNPs for a long period of time. The differences in hydroxyl group position of those three compounds showed the different performance of AuNPs, as well as the size and stability of the materials.

The AuNPs were obtained through several rounds of optimizations and the first optimization conducted in this research was the optimization of pH. Fig. 1 reveals that the AuNPs capped by either *o*-hydroxybenzoic acid, *m*-hydroxybenzoic acid, or *p*-hydroxybenzoic acid were only formed at pH 12. It can be seen from characteristic Surface Plasmon Resonance (SPR) of AuNPs in the range of 500–560 nm [14]. Except for pH 12, SPR characteristic peak belonging to AuNPs was not observed for another pH. This result is similar to the study reported by Qin et al. where the size and shape of nanoparticles were obtained by varying the pH of the solution. They also found that the size of nanoparticles was smaller and the shape was more rounded when the pH was increased [15]. The basic condition makes the capping agent to carry a negative charge (R-COO^- and

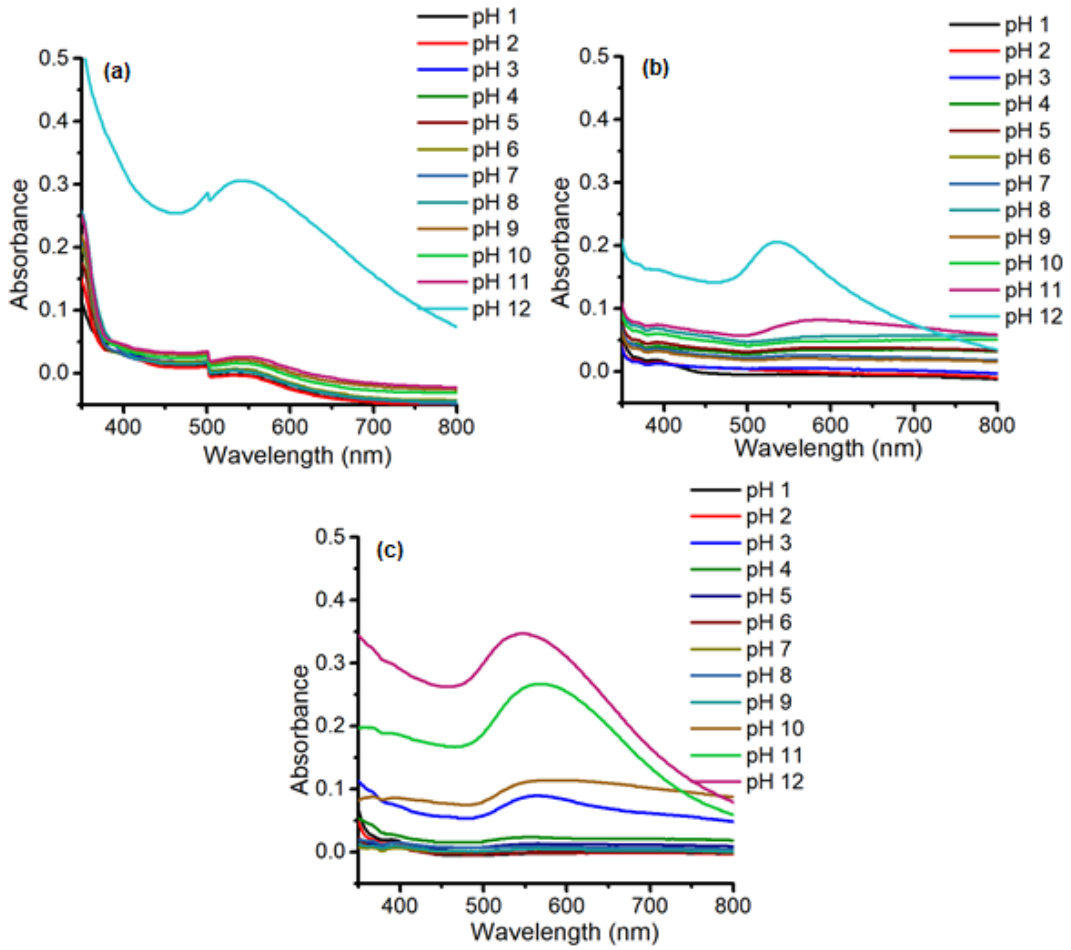

Fig 1. SPR spectra of AuNPs using different pH of 0.01 M capping agents, (a) *o*-hydroxybenzoic acid, (b) *m*-hydroxybenzoic acid, (c) *p*-hydroxybenzoic acid, 50 ppm Au^{3+}, and 1 h of reaction time

R-O$^-$) and this capping agent binds and stabilizes the metal. AuNPs also have a different color from their bulk form. AuNPs were red wine to purplish blue depending on the size of obtained gold nanoparticles [16]. The clear color of the solution at pH 1–11 indicated that no AuNPs was formed.

The next optimization was the reaction time conducted at pH 12 using 0.01 M capping agent and 50 ppm $[AuCl_4]^-$. The result showed that the optimum reaction time for the synthesis of AuNPs using *o*-hydroxy benzoic acid, *m*-hydroxybenzoic acid and *p*-hydroxybenzoic acid as capping agents was 20, 10 and 30 min, respectively (Fig. 2). AuNPs capped by *p*-hydroxybenzoic acid required a longer synthesis time than other capping agents. The speed of formation of AuNPs listed in descending order is as follows: *m*-hydroxybenzoic acid > *o*-hydroxybenzoic acid > *p*-hydroxybenzoic acid.

The concentration of the Au^{3+} solution is one of the most important factors to synthesize AuNPs. The size and stability of nanoparticles are influenced by the initial concentration of metal [17]. In this research, both Au^{3+}

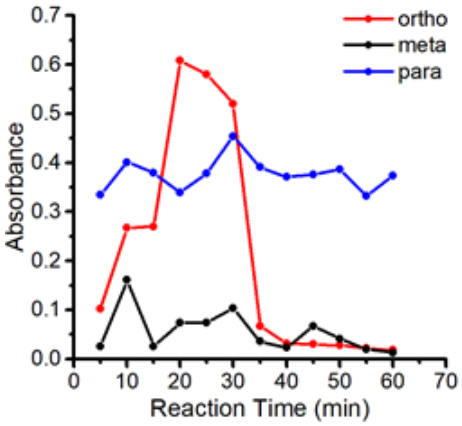

Fig 2. The plot of the absorbance of AuNPs versus reaction time during synthesis

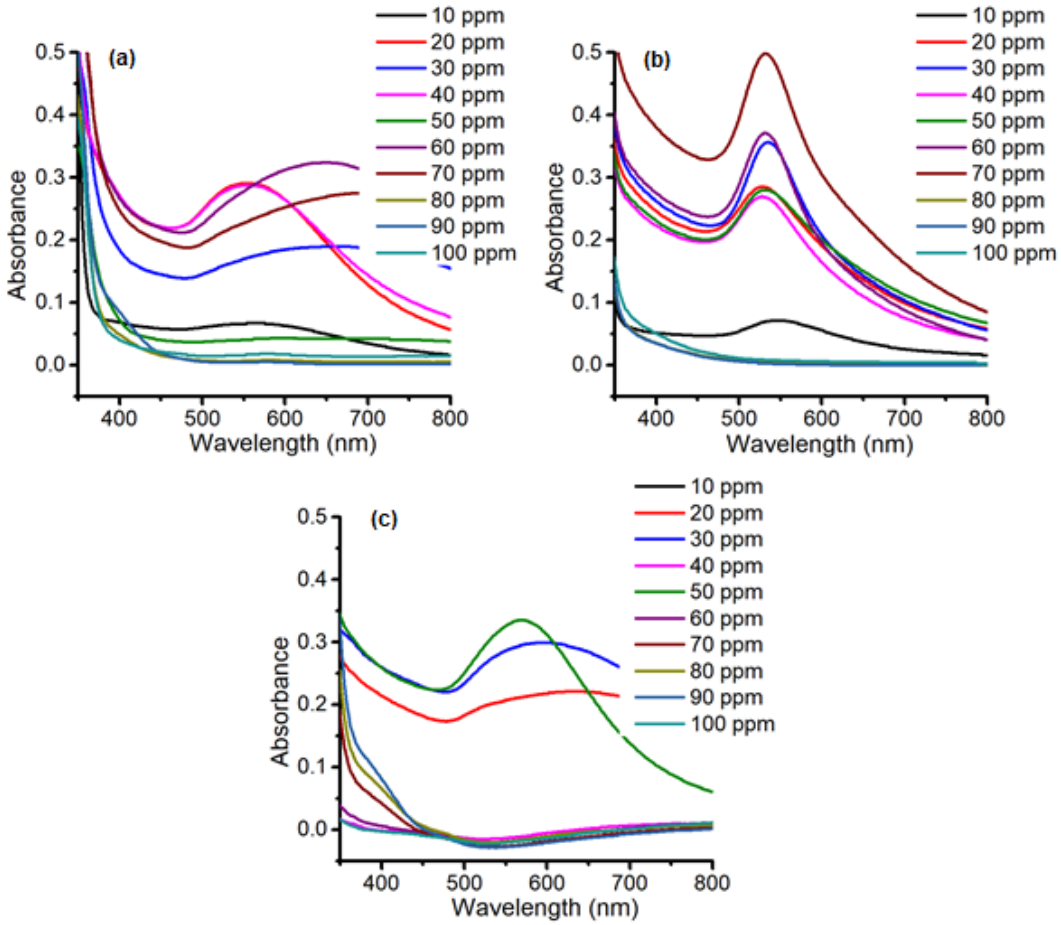

Fig 3. SPR spectra of AuNPs at different concentration of Au^{3+}, 0.01 M capping agents, 1 h reaction time, (a) *o*-hydroxybenzoic acid, (b) *m*-hydroxybenzoic acid, (c) *p*-hydroxybenzoic acid

solution and capping agent concentrations were varied. By increasing the concentration of the Au^{3+} solution, the absorbance of AuNPs was increased. It means that the number of AuNPs product increased until it reached optimum concentration (Fig. 3). When the concentration of the Au^{3+} solution was increased beyond 70 ppm in the synthesis of AuNPs by using *o*-hydroxybenzoic acid, the color of solutions became clear and a peak at 527–544 nm in their SPR spectra was not observed. This result indicated that the AuNPs were not formed under such condition. Concentrations of Au^{3+} solutions higher than 70 ppm decreased the ability of the capping agent to reduce and stabilize the Au metal due to the high number of Au metal in the solution. Consequently, the AuNPs were not formed. This phenomenon also happened in the synthesis of AuNPs when using *m*-hydroxybenzoic acid and *p*-hydroxybenzoic acid as capping agents. The optimum concentration of the Au^{3+} solution to form AuNPs for *m*-hydroxybenzoic acid and *p*-hydroxybenzoic acid as capping agents was achieved at 20 ppm and 50 ppm, respectively. It means that the number of AuNPs decreased when the concentration of the Au^{3+} solution was increased beyond the optimum condition. In addition to the optimization of the Au^{3+} concentration, optimization of capping agent concentration was also carried out in this research. The optimum concentration of capping agent (*o*-hydroxybenzoic acid, *m*-hydroxy benzoic acid, and *p*-hydroxybenzoic acid) to form the AuNPs was 0.01 M. When their concentration was increased, the AuNPs were not formed.

Characterization of AuNPs

The formation of AuNPs was confirmed by X-ray diffraction. XRD pattern of AuNPs (Fig. 4) showed several diffraction peaks of AuNPs-ortho observed at 2θ of 38.01, 44.24, 64.36, and 77.27°, which can be attributed to (111), (200), (220), and (311) planes of the face-centered cubic (fcc) of Au^0, respectively. The obtained data matched well with the JCPDS no 04-0784, which suggests that crystalline AuNPs were formed. The XRD pattern of AuNPs-meta and AuNPs-para exhibited similar diffraction peaks at 2θ at 38.13, 44.15, 64.44, 75.58, 38.14, 44.03, 64.54, and 77.47°, respectively. The

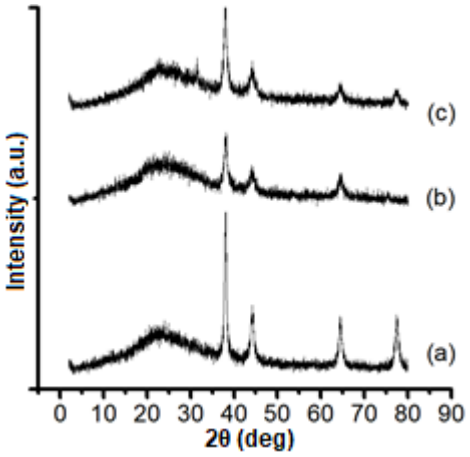

Fig 4. XRD patterns of AuNPs capped by benzoic acid derivatives, (a) AuNPs-ortho, (b) AuNPs-meta, (c) AuNPs-para

XRD pattern of AuNPs-ortho indicated that the AuNPs-ortho have greater crystallinity than other AuNPs. Therefore, the AuNPs-ortho were considered to have the most effective redox reaction than those produced using *m*-hydroxybenzoic acid and *p*-hydroxy benzoic acid.

The particle shape and morphology of AuNPs were analyzed by TEM and the result is presented in Fig. 5. The AuNPs-ortho have spherical, triangular, and hexagonal shape with varied size. It is different from AuNPs-para and AuNPs-meta which have a spherical shape. The variation in size and shape of AuNPs-ortho was caused by the high Au^{3+}/capping agent ratio in the synthesis of AuNPs-ortho [18]. AuNPs-meta and AuNPs-para have a spherical shape because their Au^{3+}/capping agent ratio is relatively low.

TEM images depict that the AuNPS-ortho did not aggregate, but the particles of AuNPs-meta completely aggregated, and AuNPs-para only partially aggregated (Fig. 5). The TEM results are supported by results of PSA showing the size distribution of AuNPs-ortho, AuNPs-meta, and AuNPs-para being 61.6, 132.6, and 85.9 nm, respectively. The AuNPs-meta was larger in size than other AuNPs due to aggregation. This observed aggregation of AuNPs was related to their stability. The stability of the AuNPs suspension was often described by their zeta potential [19]. The greater zeta potential value indicates the smaller size and higher stability of AuNPs. From Table 1, AuNPs-ortho has the highest potential

zeta value than the AuNPs-para and AuNPs-meta. Therefore, the size of AuNPs-ortho was the smallest and most stable than other AuNPs.

The absorbance of AuNPs-ortho was relatively stable and only changed slightly after five months (Fig. 6). This was different when compared to other capping agents, where their absorbance drastically decreased after

Table 1. Zeta potential and particle size of AuNPs

System	Zeta potential (mV)	Particle Size (nm)
AuNPs-ortho	-44.6	61.6
AuNPs-meta	-26.4	132.6
AuNPs-para	-31.3	85.9

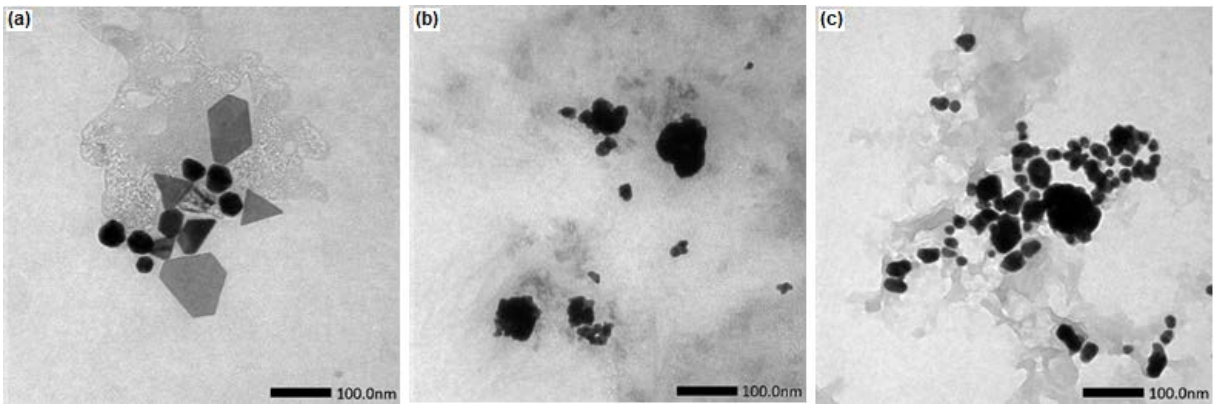

Fig 5. TEM images of (a) AuNPs-ortho, (b) AuNPs-meta, and (c) AuNPs–para

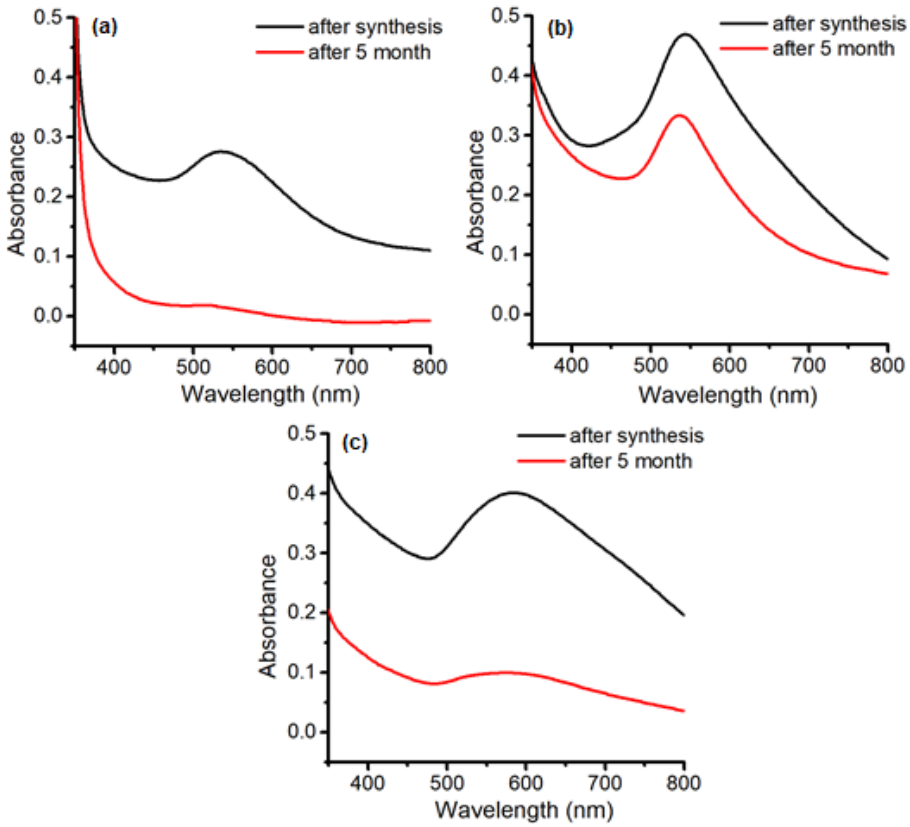

Fig 6. SPR spectra of the stability of AuNPs after 5 months incubation at room temperature (a) *o*-hydroxybenzoic acid, (b) *m*-hydroxybenzoic acid, (c) *p*-hydroxybenzoic acid

five months. The AuNPs-meta and AuNPs-para solution had precipitated after five months, and it means that the AuNPs produced using *m*-hydroxybenzoic acid and *p*-hydroxybenzoic acid as caping agents had aggregated, and they were easily settled. The order of stability of the produced AuNPs based on the position of the hydroxyl group is as follows: *o*-hydroxybenzoic acid > *p*-hydroxy benzoic acid > *m*-hydroxybenzoic acid.

AuNPs-ortho and AuNPs-para were more stable than AuNPs-meta. It was caused by the resonance of *o*-hydroxybenzoic acid and *p*-hydroxybenzoic acid structure which delocalized their negative charge to their carboxylic group. Their resonance structure in the redox reaction could encourage the formation of quinone, which could effectively form AuNPs with high stability (Fig. 7). However, the experimental data showed that the AuNPs-ortho were more stable than AuNPs-para. The stability of AuNPs-ortho was due to the three oxygen atoms from *o*-hydroxybenzoic acid which capped the Au^0 by electrostatic attraction, and this phenomenon consequently stabilized the AuNPs. On the other hand, the *p*-hydroxybenzoic acid only had two oxygen atoms which stabilized the Au^0 (Fig. 8). However, the resonance structure of *m*-hydroxybenzoic acid did not

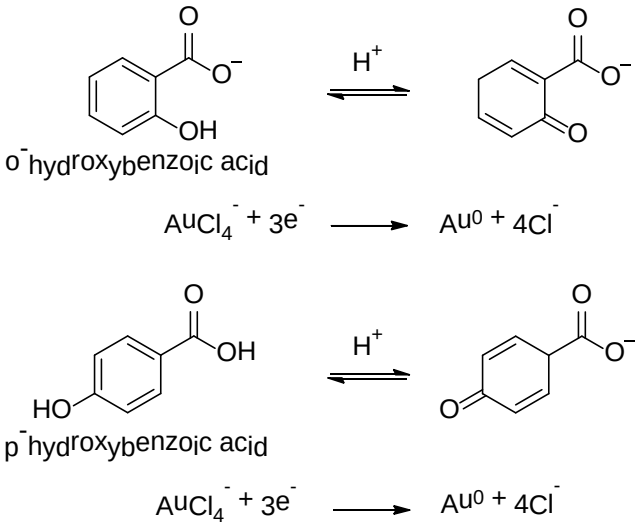

Fig 7. Reduction mechanism of Au^{3+} to Au^0 by *o*-hydroxybenzoic acid and p-hydroxybenzoic acid

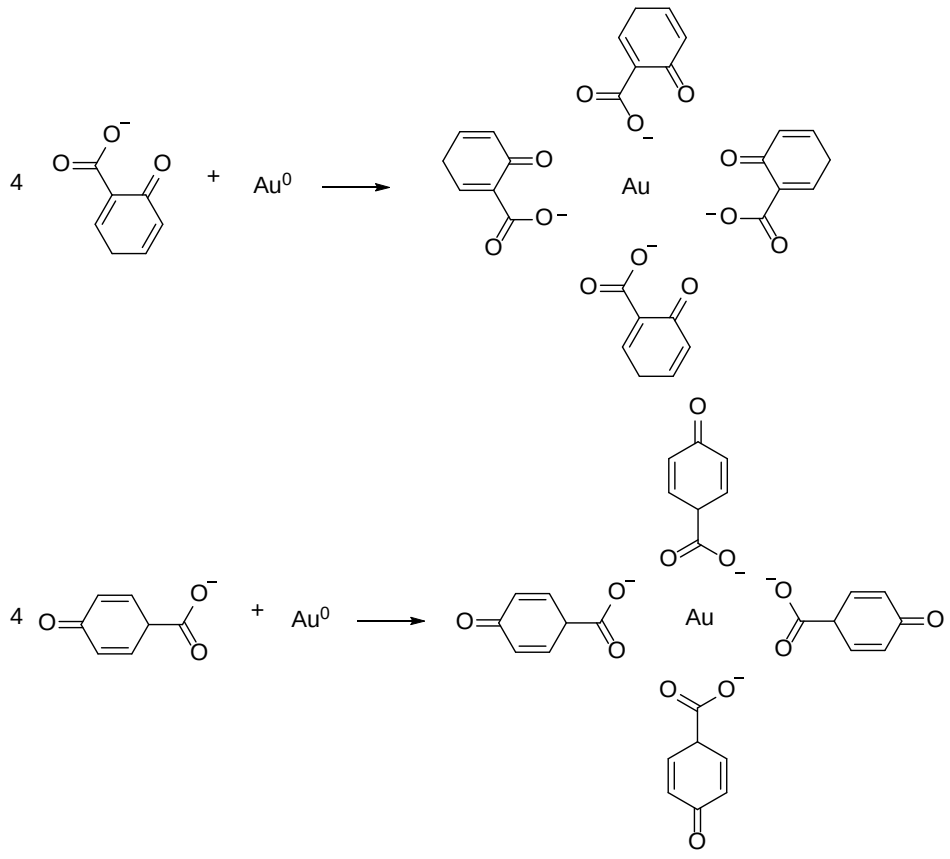

Fig 8. Stabilization mechanism of AuNPs by *o*-hydroxybenzoic acid and *p*-hydroxybenzoic acid

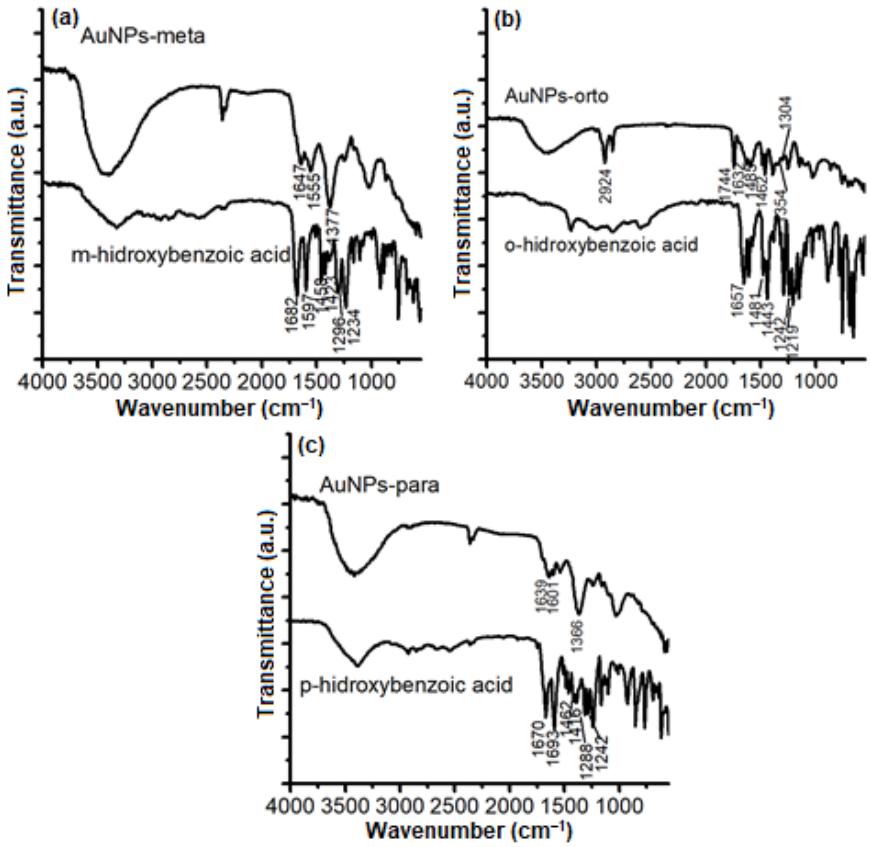

Fig 9. FTIR Spectra of (a) AuNPs-ortho and ortho-hydroxybenzoic acid, (b) AuNPs-meta and meta-hydroxybenzoic acid, (c) AuNPs-para and para-hydroxybenzoic acid

delocalize their negative charge to their carboxylic group. This did not encourage the formation of quinone and resulted in the formation of AuNPs with lower stability.

The stability of AuNPs-ortho was also indicated by its color in solution form. The color of AuNPs solution synthesized using *o*-hydroxybenzoic acid as a capping agent was red, but other capping agents gave purplish-blue color to the AuNPs solution. The red color of the AuNPs solution indicated the formation of smaller sized AuNPs than the purplish-blue ones. The smaller sized AuNPs do not easily aggregate and settle, hence, are more stable as compared to larger sized AuNPs. Gosh et al. summarized the particle size relationship in relation to the SPR spectra. The higher the wavelength of the peak in the SPR spectra, the larger their particles size tend to be, as indicated by the change in the AuNPs color from red to blue [20]. This was similar to a description by Chao et al. [19] which specified that the size pf AuNPs at 520 nm was 13 nm. When the SPR wavelength undergoes a redshift, the particles size was increased accompanied by a color change to blue [21].

FTIR characterization shows that benzoic acid derivatives capped the AuNPs (Fig. 9). Through IR characterization, the group will act as a reducing agent or stabilizing agent was identified. The IR spectrum of *o*-hydroxybenzoic acid (Fig. 9(a)) revealed an absorption peak which corresponded to a C=O stretching vibration that appeared at 1657 cm^{-1}. This absorption peak shifted from 1657 to 1632 cm^{-1} due to the presence of an electrostatic bond of C=O with Au metal [22]. The IR spectrum for o-hydroxybenzoic acid at 1481 and 1443 cm^{-1} w*as* confirmed as C=C stretching vibration of aromatic carbon, and they shifted to 1485 and 1462 cm^{-1} in AuNPs-ortho [23]. The most interesting thing was the presence of a new absorption peak at 1744 cm^{-1} in the IR spectrum of AuNPs-ortho, indicative of a C=O stretching vibration of ketone from the oxidation of a hydroxyl group of *o*-hydroxybenzoic acid. When the

hydroxyl group was oxidized to a ketone group, the Au^{3+} was reduced to Au^0 (Fig. 7). When the hydroxyl group acted as a reducing agent, it was predicted that the carboxylic group had functioned as the stabilizing agent. In IR spectra of AuNPs-meta and AuNPs-para (Fig. 9(b) and 9(c)), the absorption peak of C=O stretching vibration shifted to 1647 and 1601 cm^{-1}, respectively. In addition, the IR spectra of AuNPs-meta and AuNPs-para also exhibited an absorption peak for the stretching vibrations of C=C aromatics, C-O, and C-OH that shifted around 1400, 1290, and 1240 cm^{-1}, respectively. However, an absorption peak at 1744 cm^{-1} which corresponds to the C=O stretching vibration of a ketone group was absent in the IR spectra of AuNPs-meta and AuNPs-para. This was because of the lower ability of the *m*-hydroxybenzoic acid and *p*-hydroxybenzoic acid to reduce Au^{3+}, as described in the above reaction mechanism (Fig. 8). Thus, the FTIR data corresponded well with results of TEM, PSA, and potential zeta for the formation of the three AuNPs.

■ CONCLUSION

The AuNPs were easily synthesized using the derivative compounds of hydroxybenzoic acid i.e. *o*-hydroxybenzoic acid, *m*-hydroxybenzoic acid, and *p*-hydroxybenzoic acid, which acted as both reducing and stabilizing agents at pH 12. To be able to synthesize AuNPs, concentrations of 70, 20, and 50 ppm of Au^{3+} for *o*-hydroxybenzoic acid, *m*-hydroxybenzoic acid, and *p*-hydroxybenzoic acid were needed, respectively. The heating time to synthesize the AuNPs using capping agents, *o*-hydroxybenzoic acid, *m*-hydroxybenzoic acid, and *p*-hydroxybenzoic acid, was optimum at 20, 10, and 30 min, respectively. Results by UV-Vis, FTIR, TEM, XRD, Zeta Potential, and PSA characterization proved that *o*-hydroxybenzoic acid resulted in the most stable synthesized AuNPs. The use of *o*-hydroxybenzoic acid to cap AuNPs demonstrated the highest stability after 5 months of incubation at room temperature, a compared to other capping agents. In conclusion, utilization of $[AuCl_4]^-$ as a precursor in conjunction with *o*-hydroxybenzoic acid as the capping agent to synthesize AuNPs, resulted in the formation the most stable nanoparticles.

■ ACKNOWLEDGMENTS

The authors would like to thank the Ministry of Research and Higher Education of the Republic of Indonesia, which supported this study through a scholarship of Master Education Program Leading to Doctoral Degree for Excellent Graduates (PMDSU) (1511/E4.4/2015).

■ REFERENCES

[1] Shellaiah, M., Simon, T., Sun, K.W., and Ko, F.H., 2016, Simple bare gold nanoparticles for rapid colorimetric detection of Cr^{3+} ions in aqueous medium with real sample applications, *Sens. Actuators, B*, 226, 44–51.

[2] Li, J., Wang, X., Huo, D., Hou, C., Fa, H., Yang, M., and Zhang, L., 2017, Colorimetric measurement of Fe^{3+} using a functional paper-based sensor based on catalytic oxidation of gold nanoparticles, *Sens. Actuators, B*, 242, 1265–1271.

[3] Shrivas, K., Shankar, R., and Dewangan, K., 2015, Gold nanoparticles as a localized surface plasmon resonance based chemical sensor for on-site colorimetric detection of arsenic in water samples, *Sens. Actuators, B,* 220, 1376–1383.

[4] Turkevich, J., Stevenson, P.C., and Hillier, J., 1951, A study of the nucleation and growth process in the synthesis of colloidal gold, *Discuss. Faraday Soc.*, 11, 55–75.

[5] Walekar, L.S., Pawar, S.P., Gore, A.H., Suryawanshi, V.D., Undare, S.S., Anbhule, P.V., Patil, S.R., and Kolekar, G.B., 2016, Surfactant stabilized AgNPs as a colorimetric probe for simple and selective detection of hypochlorite anion (ClO^-) in aqueous solution: Environmental sample analysis, *Colloids Surf., A*, 491, 78–85.

[6] Bialik-Wąs, K., Tyliszczak, B., Sobczak-Kupiec, A., Malina, D., and Piątkowski, M., 2012, The effect of dispersant concentration on properties of bioceramic particles, *Dig. J. Nanomater. Biostruct.*, 7 (1), 361–366.

[7] Zhao, P., Li, N., and Astruc, D., 2013, State of the art in gold nanoparticle synthesis, *Coord. Chem. Rev.*, 257 (3-4), 638–665.

[8] Kimling, J., Maier, M., Okenve, B., Kotaidis, V., Ballot, H., and Plech, A., 2006, Turkevich method for gold nanoparticle synthesis, *J. Phys. Chem. B*, 110 (32), 15700–15707.

[9] Fitriyana, F., and Kurniawan, F., 2015, Polyaniline-invertase-gold nanoparticles modified gold electrode for sucrose detection, *Indones. J. Chem.*, 15 (3), 226–233.

[10] Roto, R., Marcelina, M., Aprilita, N.H., Mudasir, M., Natsir, T.A., and Mellisani, B., 2017, Investigation on the effect of addition of Fe^{3+} ion into the colloidal AgNPs in PVA solution and understanding its reaction mechanism, *Indones. J. Chem.*, 17 (3), 439–445.

[11] Indumathy, R., Sreeram, K.J., Sriranjani, M., Aby, C.P., and Nair, B.U., 2010, Bifunctional role of thiosalicylic acid in the synthesis of silver nanoparticles, *Mater. Sci. Appl.*, 1 (5), 272–278.

[12] Gusrizal, G., Santosa, S.J., Kunarti, E.S., and Rusdiarso, B., 2016, Dual function of *p*-hydroxy benzoic acid as reducing and capping agent in rapid and simple formation of stable silver nanoparticles, *Int. J. ChemTech Res.*, 9 (9), 472–482.

[13] Gusrizal, G., Santosa, S.J., Kunarti, E.S., and Rusdiarso, B., 2017, Synthesis of silver nanoparticles by reduction of silver ion with *m*-hydroxybenzoic acid, *Asian J. Chem.*, 29 (7), 1417–1422.

[14] Krishnamurthy, S., and Yun, Y.S., 2013, Recovery of microbially synthesized gold nanoparticles using sodium citrate and detergents, *Chem. Eng. J.*, 214, 253–261.

[15] Qin, Y., Ji, X., Jing, J., Liu, H., Wu, H., and Yang, W., 2010, Size control over spherical silver nanoparticles by ascorbic acid reduction, *Colloids Surf., A*, 372, 172–176.

[16] Priyadarshini, E., and Pradhan, N., 2017, Gold nanoparticles as efficient sensors in colorimetric detection of toxic metal ions: A review, *Sens. Actuators, B*, 238, 888–902.

[17] Liu, J., Lee, J.B., Kim, D.H., and Kim, Y., 2007, Preparation of high concentration of silver colloidal nanoparticles in layered laponite sol, *Colloids Surf., A*, 302 (1-3), 276–279.

[18] Kaviya, S., and Prasad, E., 2014, Sequential detection of Fe^{3+} and As^{3+} ions by naked eye through aggregation and dis-aggregation of biogenic gold nanoparticles, *Anal. Method*, 7 (1), 168–174.

[19] Litvin, V.A., and Minaev, B.F., 2014, The size-controllable, one-step synthesis and characterization of gold nanoparticles protected by synthetic humic substances, *Mater. Chem. Phys.*, 144 (1-2), 168–178.

[20] Ghosh, S.K., Pal, A., Kundu, S., Nath, S., and Pal, T., 2004, Fluorescence quenching of 1-methyl aminopyrene near gold nanoparticles: Size regime dependence of the small metallic particles, *Chem. Phys. Lett.*, 395 (4-6), 366–372.

[21] Li, S., Li, Y., Cao, J., Zhu, J., Fan, L., and Li, X., 2014, Sulfur-doped graphene quantum dots as a novel fluorescent probe for highly selective and sensitive detection of Fe^{3+}, *Anal. Chem.*, 86 (20), 10201–10207.

[22] Sánchez-Cortés, S., and García-Ramos, J.V., 2000, Adsorption and chemical modification of phenols on a silver surface, *J. Colloid Interface Sci.*, 231 (1), 98–106.

[23] Alvarez-Ros, M.C., Sánchez-Cortés, S., and García-Ramos, J.V., 2000, Vibrational study of the salicylate interaction with metallic ions and surfaces, *Spectrochim. Acta, Part A*, 56 (12), 2471–2477.